A novel MEMS inertial sensor with enhanced sensing capacitors*

Dong Linxi(董林玺)[1, †], Yan Haixia(颜海霞)[2], Huo Weihong(霍卫红)[1], Xu Li(许立)[1],
Li Yongjie(李永杰)[1], and Sun Lingling(孙玲玲)[1]

(1 Key Laboratory of RF Circuits and Systems, Ministry of Education, Hangzhou Dianzi University, Hangzhou 310018, China)

(2 Toshiba Hydro-Electro Equipments Company, Hangzhou 311504, China)

Abstract: A novel MEMS inertial sensor with enhanced sensing capacitors is developed. The designed fabricated process of the sensor is a deep RIE process, which can increase the mass of the seismic to reduce the mechanical noise, and the designed capacitance sensing method is changing the capacitance area, which can reduce the air damping between the sensing capacitor plates and reduce the requirement for the DRIE process precision, and reduce the electronic noise by increasing the sensing voltage to improve the resolution. The design and simulation are also verified by using the FEM tool ANSYS. The simulated results show that the transverse sensitivity of the sensor is approximately equal to zero. Finally, the fabricated process based on silicon–glass bonding and the preliminary test results of the device for testing grid capacitors and the novel inertial sensor are presented. The testing quality factor of the testing device based on the slide-film damping effect is 514, which shows that the enhanced capacitors can reduce mechanical noise. The preliminary testing result of the sensitivity is 0.492 pf/g.

1. Introduction

MEMS capacitive sensors have been increasingly popular in recent years due to their process compatibility with most mechanical structures, their high sensitivity, and their low temperature drift. Some applications, such as high precision inertial navigation, seismic sensing for geophysical and oil-field applications, earthquake prediction, and shock and vibration detection, need high sensitivity and resolution, which are limited mainly by the noise level, including the mechanical noise caused by the Brownian motion of air around the capacitor[1] and electrical noise caused by the noise of the signal detection circuitry[2]. Capacitive MEMS accelerometers can be implemented by using a variety of surface and bulk micromachining technologies. In surface micro-machined devices, the thickness of the deposited layer and, hence, the proof mass are small, limiting the resolution of the micro-accelerometers[3]. On the other hand, bulk micromachining, for example the DRIE process, provides larger proof mass and larger capacitive area, which lead to a higher resolution and a greater sensitivity. When the comb capacitances of MEMS comb capacitive accelerometers are fabricated by using the DRIE process, the combs are usually not parallel because of the complicated process factors, which affects the reliable working range and the linearity of the sensors[4]. As it is well-known, for capacitive sensing, a certain form of alternative electric test signal is usually necessary for detecting the variation of the capacitance; in this situation, the sensor is influenced by an electrostatic force, an inertial force, a damping force, a spring force, etc. In case of a pull-in failure, the seismic mass of the inertial sensor is pulled into permanent contact with the static electrode and re-mains there until the power supply of the sensor is reset, which restricts the application of the method reducing the electrical noise by increasing the sensing voltage[5].

In this paper, aiming at the disadvantage of comb capacitive MEMS accelerometers, a novel micro-accelerometer, whose damping is mainly due to slide film air damping, is designed and fabricated in effort to reduce the mechanical noise and increase the resolution. The capacitance is sensed mainly by a variable area, which can increase the voltage of the electronic testing signal to reduce the circuit noise and may reduce the precision requirements of the DRIE process.

2. Device design and analysis

2.1. Mechanical noise

The mechanical noise, which is generated by the Brownian motion of the air around the sense element, is one of the most important factors restricting the improvement of the resolution of MEMS capacitive accelerometers. The air damping can be distinguished as squeezed-film air damping and slide-film air damping, depending on the MEMS device structure. For the parallel plate capacitor structure, the squeezed-film damping and the slide-film damping for ambient pressure at room temperature can be calculated by[6]

$$c_{\text{rec}} = \frac{\mu L B^3}{h^3}\left(1 - \frac{192}{\pi^5}\frac{B}{L}\sum_{n=1,3,5}^{\infty}\frac{1}{n^5}\tanh\frac{n\pi L}{2B}\right),$$

$$c_{\text{sd}} = \frac{A\mu}{\delta}\frac{\sinh 2\tilde{d} + \sin 2\tilde{d}}{\cosh 2\tilde{d} - \cos 2\tilde{d}},$$

(1)
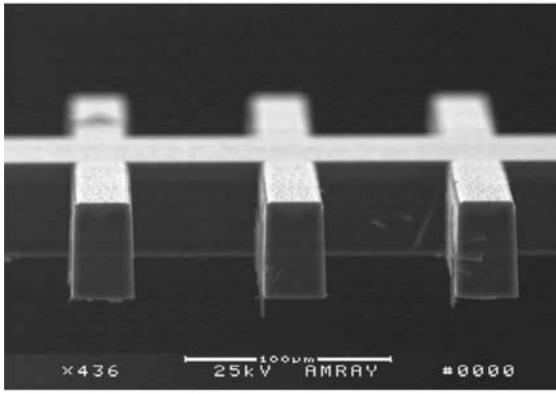
Fig. 1. SEM picture of the cross section of non-parallel combs of the movable seismic mass.

where B is the width of the capacitor plate, L is the length, μ is the viscosity coefficient of air, h is the distance between the capacitor plates, $\delta = \sqrt{2\mu/\rho\omega}$ is the effective decay distance, A is the overlap area, $\tilde{d} = d/\delta$, d is the distance between the electrodes. According to the definition of the quality factor of $Q = m\omega_r/c$, where m is the mass of the seismic, c is the coefficient of the air damping force, and ω_r is the resonant frequency, the quality factor can be improved by increasing the mass or reducing the air damping of the sensor. According to the analysis of Gabrieson[1], the effect of air damping on a MEMS accelerometer can be expressed by

$$\overline{a_m} = \sqrt{\frac{4k_B T \omega_n}{mQ}}, \tag{2}$$

where k_B, T, and ω_n are the Boltzmann constant, the absolute temperature, and the natural frequency, respectively. The equation shows that the bulk-silicon micromachining process, which leads to a relatively large mass of the seismic, can reduce the mechanical noise. Since the squeezed-film damping is usually larger than the slide-film damping, the designed accelerometer is based on slide-film damping in order to improve the resolution.

2.2. Electrical noise

The capacitive accelerometer has a high precision, but its sensing circuit is very complicated. One solution is to use a high frequency carrier wave signal when using the MEMS sensing capacitors in order to modulate the acceleration signal. Afterwards, the signal is amplified and demodulated. In this case, the electrical noise is determined mainly by the noise in the frond-end preamplifier. The electrical noise can be expressed by[2]

$$\overline{a_e} = \sqrt{\frac{\alpha}{C + C_p} \frac{\omega_n^2}{V_s} \overline{v_e}}, \tag{3}$$

where α is a constant related to the size of the sensor, C is the sensing capacitance of the sensor, C_p is the parasitical capacitance, V_s is the voltage of the test signal, and $\overline{v_e}$ is the voltage of the input noise. It can be seen from the above equation that the electronic noise of the sensing circuit can be reduced by increasing the sensing capacitance or the voltage amplitude of the test signal, when designing the capacitive inertial sensor.
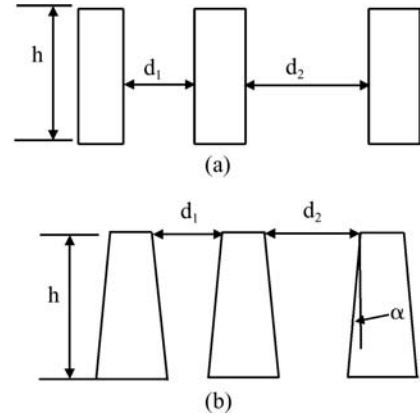
2.3. Effects of non-parallel comb capacitances on the capacitive inertial sensor

The combs of the comb capacitive inertial sensors fabricated by deep reactive ion etching are usually not parallel, as shown in Fig. 1. In Ref. [4], the effects of non-parallel combs on the reliable operation range for step and pulse signals in three capacitive configurations are investigated, when alternative electronic test signals are applied to the sensors for detecting the variation of the capacitance. Results show that for a step inertial signal of a low decline angle of 0.5°, the reliable operation ranges of the sensors having a single-sided structure, a double-sided structure and a double-sided structure with feedback voltage are reduced to 0.34, 0.44, and 0.54 compared to the ones whose comb electrodes are parallel, respectively. For a pulse inertial signal, the reliable operation ranges with a single-sided structure and a double-sided structure are reduced to 0.45 and 0.56, respectively. For a double-sided capacitive sensor with feedback voltage, the range is reduced to 0.95 as the angle is changed from 0.1° to 0.15°, which shows that the effects of the non-parallel structure can not be ignored. In Ref. [8], the effects of non-parallel combs on the inertial pulse response of an MEMS capacitive accelerometer are investigated, considering the damping force in a low vacuum environment. Results show that a non-parallel comb factor induced by the DRIE process influences the displacement caused by an outside acceleration and degrades the linearity range of the inertial sensors. The results also show that the effect of a non-parallel comb on the response displacement becomes more pronounced as the voltage of the test signal becomes larger. Therefore, for a comb capacitive micro-accelerometer, a high amplitude test voltage can not be used for a non-parallel comb and nonlinearity factors.

To limit the effect of the DRIE process and the nonlinearity problem at high amplitude voltages, a novel MEMS capacitive accelerometer is designed and fabricated, as shown in Fig. 2.

2.4. A novel micro-accelerometer design and analysis

The schematics of the novel capacitive micro-accelerometer are shown in Fig. 2. The micro-accelerometer is mainly composed of a single seismic mass, a supporting beam, grid strips, combs, and fingers. The sensing capacitan-
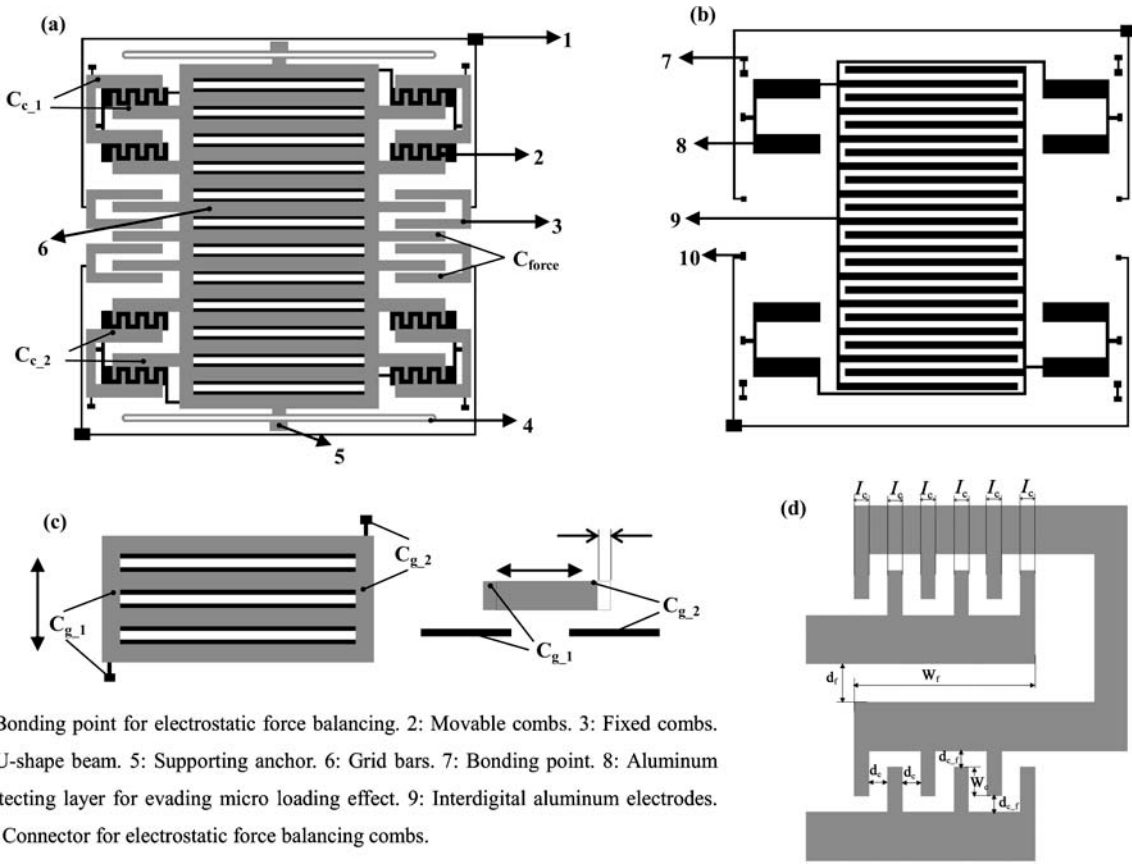
Fig. 2. Schematic pictures of the designed MEMS capacitive sensor: (a) Simplified schematic model of the sensor; (b) Simplified Al electrodes on the glass substrate; (c) Schematic model of grid shape sensing capacitors; (d) Schematic model of comb sensing capacitors.

ces include grid strip capacitances, comb capacitances, finger capacitances, and capacitances between the combs and the fingers, respectively. The sensing capacitances are increased by the novel structure design, which reduces electrical noise. The damping of the grid strip capacitances and the comb capacitances are all due to slide-film air damping, which reduces the mechanical noise. The nonlinearity induced by the electrostatic force is limited by the grid strip capacitances and the comb capacitances design, and the noise is also reduced by the increasing voltage of the test signal.

The capacitance, C_{comb}, between a pair of combs having a small tilt angle α caused by the deep RIE process can be computed by[7]

$$C_{\mathrm{comb}} = \frac{\varepsilon\varepsilon_0 w_{\mathrm{c}}}{2\alpha} \ln \frac{d}{d - 2h\tan\alpha}, \tag{4}$$

where d, ε, ε_0, h, and w_{c} are the gap between combs, the permittivity of vacuum, the relative permittivity of air, the thickness of the comb, and the overlap between the combs, respectively.

The sensing capacitance of the novel micro-accelerometer can be expressed as

$$C_0 = \varepsilon\varepsilon_0 \left(\frac{w_{\mathrm{c}}}{2\alpha} \ln \frac{d}{d - 2h\tan\alpha} + \frac{N_{\mathrm{c}} l_{\mathrm{c}} h}{d_{\mathrm{c\_f}}} - \frac{N_{\mathrm{f}} w_{\mathrm{f}} h}{d_{\mathrm{f}}} + \frac{N_{\mathrm{g}} L_{\mathrm{g}} w_{\mathrm{g}}}{d_0} \right), \tag{5}$$

where N_{c} is the number of overlapping combs, N_{f} is the number of overlapping fingers, N_{g} is the number of the gird strips, L_{g} is the length of the grid strip, and w_{g} is the width of the overlap between the grid strip and the electrode on the substrate.

According to Eq. (5), the change of the sensing capacitance can be computed by

$$\Delta C \doteq \varepsilon\varepsilon_0 w_{\mathrm{c}} \left(\frac{1}{2\alpha} \ln \frac{d}{d - 2h\tan\alpha} + \frac{N_{\mathrm{c}} l_{\mathrm{c}} h}{d_{\mathrm{c\_f}}^2} - \frac{N_{\mathrm{f}} w_{\mathrm{f}} h}{d_{\mathrm{f}}^2} + \frac{N_{\mathrm{g}} L_{\mathrm{g}}}{d_0} \right) \frac{y}{w_{\mathrm{c}}}$$

$$\text{for} \quad y \ll d_{\mathrm{f}}, d_{\mathrm{c\_f}}, \tag{6}$$

where y is the displacement generated by the external inertial signal. Equation (7) shows that the inclination of the combs induced by the deep RIE process will not cause nonlinearity changes of the sensing capacitance.

Because of the conservation of energy, the electrostatic force between combs having a small angle can be computed by

$$F_{\mathrm{comb\_e}} = -\frac{\partial E(y)}{\partial y} = -\frac{\partial \left(E_0 - \frac{1}{2} \frac{\varepsilon\varepsilon_0 y}{2\alpha} \ln \frac{d}{d - 2h\tan\alpha} V^2 \right)}{\partial y}$$

$$= \frac{1}{2} \frac{\varepsilon\varepsilon_0}{2\alpha} \ln \frac{d}{d - 2h\tan\alpha} V^2, \tag{7}$$

where E_0 is the energy of the battery. We can see from Eq. (7) that the force is independent of the overlap, y, so that the force remains constant during the movement of the seismic. If the moving direction of the combs is normal, the electrostatic force between combs with a small oblique angle is $F_{\mathrm{comb\_e}}' = \varepsilon\varepsilon_0 A V^2 / 2d(d - 2\alpha h)$, which causes a nonlinearity of the micro-accelerometer, and the oblique combs induced by the deep RIE process significantly affect the capacitance and
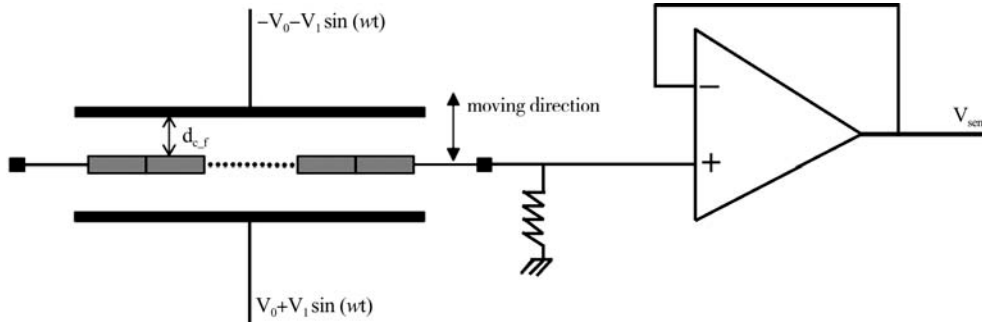
Fig. 3. Equivalent electrical model of the capacitance between combs and fingers of the sensors.
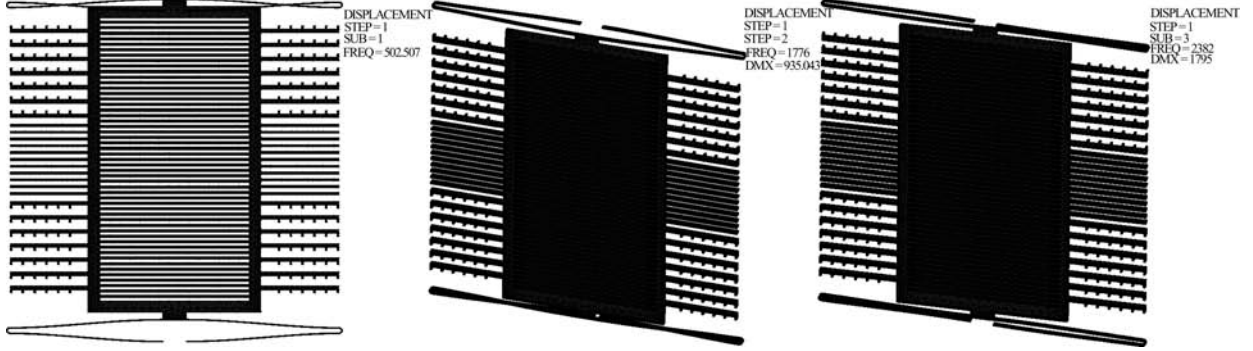
Fig. 4. The first, second, and third vibratory modes of the designed inertial sensor.

electrostatic force. Consequently, the reliable operation conditions of the micro-accelerometer are affected[4].

According to Fig. 3, the sensing voltage, V_{sen}, caused by the change of the sensing capacitor, can be computed by

$$V_{\text{sen}} = \frac{\Delta C}{C_0}(V_0 + V_1 \sin \omega t) = \beta \frac{y}{w_\text{c}}(V_0 + V_1 \sin \omega t), \quad (8)$$

where β is defined as

$$\beta = \frac{\varepsilon \varepsilon_0 w_\text{c}}{C_0} \left(\frac{1}{2\alpha} \ln \frac{d}{d - 2h\tan\alpha} + \frac{N_\text{c}l_\text{c}h}{d_\text{c\_f}^2} - \frac{N_\text{f}w_\text{f}h}{d_\text{f}^2} + \frac{N_\text{g}L_\text{g}}{d_0} \right). \quad (9)$$

Therefore, the electrostatic force between the combs and the fingers of the micro-accelerometer is obtained by

$$\begin{aligned} F_\text{c\_f} = \frac{\varepsilon \varepsilon_0 A_\text{c\_f}}{2d_\text{c\_f}^2} & \left[\frac{(V_0 + V_1 \sin \omega t - V_\text{sen})^2}{(1 - \tilde{y})^2} \right. \\ & \left. - \frac{(V_0 + V_1 \sin \omega t + V_\text{sen})^2}{(1 + \tilde{y})^2} \right], \end{aligned} \quad (10)$$

where $\tilde{y} = y/w_\text{c}$. According to Eq. (10) and the analysis of the double-sided driving with feedback voltage in Ref. [8], the electrostatic force between the combs and the fingers leads to a force balancing. So, the design can increase the reliable operation range and the linearity of MEMS inertial sensors.

2.4.1. Mode analysis

The vibration modes of the novel micro-accelerometer, which is simulated by using the FEM tool ANSYS, is shown in Fig. 4. The resonant frequencies of the first, second, and third modes are 502, 1776, and 2302 Hz, respectively. When an acceleration of 1 g is applied to the accelerometer in the sensing direction, the caused displacement is 0.99 μm.

2.4.2. Strength analysis

To confirm whether the micro-accelerometer is destroyed or not when a large accidental shock is applied to the seismic, an FEM simulation is used. Overloading heaves, as shown in Fig. 7, have been designed in the sensitive direction for protecting the frame when the accelerometer is shocked by the large inertial signal. For the non-sensitive directions z and x axis, the maximum stresses, which are distributed in the fringes of the U-shape beams, are 722 and 38 MPa, for the case that the seismic is shocked by a 1000 g acceleration in the z direction and the x direction, respectively. The stress distribution is shown in Fig. 5. The results show that the designed sensor can sustain a 1000 g acceleration shock when the fracture stress of silicon is 1.3 GPa[9].

2.5. Analysis of the transverse sensitivity

The output signal in the y sensitive direction, which is affected by the signals from the x and z directions, can be expressed by

$$V_{\text{out\_y}} = s_y a_y + s_{xy} a_x + s_{zy} a_z,$$

where s_y is the sensitivity in the y direction, and s_{xy} and s_{zy} are the transverse sensitivities in the xy directions and in the zy directions, respectively.

To simulate the transverse sensitivity of the novel micro-accelerometer in the y sensitive direction, the following method is used: a 1 g acceleration is applied both in the y- and x-direction. The maximum displacements of the movable mass in the y, x, and z directions are analyzed by ANSYS; a 2 g acceleration is applied in the x-direction, while maintaining the 1 g acceleration in the y direction. The maximum displacements in the x, y, and z direction are analyzed by AN-SYS. Afterwards, the transverse sensitivity can be computed
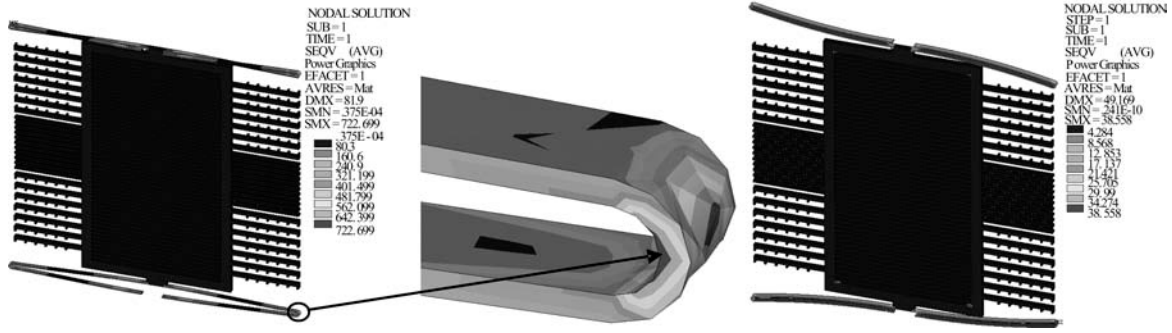
Fig. 5. Results of the strength obtained with the simulation tool ANSYS.
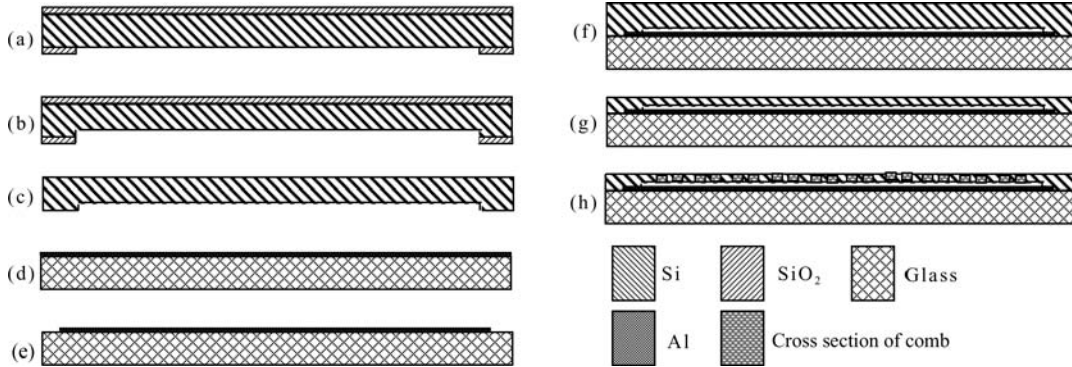
Fig. 6. Fabrication process flow of the designed inertial sensor: (a) The SiO$_2$ surface layer on the silicon wafer is first removed by HF to etch a suspending area; (b) A silicon wafer with thermal SiO$_2$ is etched to form a suspending cavity; (c) The SiO$_2$ on the silicon is entirely removed; (d) Aluminum is sputtered onto Pyrex 7740 glass substrate; (e) Aluminum interdigitated electrodes are patterned on the Pyrex 7740 glass wafer; (f) The silicon and the glass wafer are then anodically bonded; (g) The silicon on the glass is thinned down and polished to an appropriate thickness; (h) The photo resist is patterned as a mask and a deep RIE process is used to etch through the silicon wafer and release the micro-accelerometer structure.

Table 1. FEM results of the cross effect of the sensor.

Displacement simulated by FEM		Δx	Δy	Δz (μm)
$a_x = 1$ g	$a_y = 1$ g	0.0033494	0.98856	–
$a_x = 2$ g	$a_y = 1$ g	0.0066972	0.98876	–
$a_z = 1$ g	$a_y = 1$ g	–	0.98881	0.077713
$a_z = 2$ g	$a_y = 1$ g	–	0.98800	0.15540

Table 2. Geometric characteristic of the sensor.

Geometric characteristic	Designed value
Structure thickness	75 μm
Size of the chip	$4960 \times 5200 \times 75 \ \mu$m^3
Distance to substrate	4 μm
Gap between combs	3 μm

by $a = k\Delta x/m$, and the effect on the output voltage can be computed by the above equation. The simulated results are shown in Table 1. It is seen from Table 1 that the transverse displacements of the *y* axis in the *x* and *z* directions are almost equal to 0. The simulation error in Table 1 is mainly due to the granularity of the FEM grid.

3. Microfabrication process and preliminary testing

A double-side, polished N-type (100) low resistivity silicon and Pyrex glass wafers are used to fabricate the micro-accelerometer by using a bulk micromachining process. The process flow is shown in Fig. 6. SEM pictures of the micro-accelerometer are shown in Fig. 7. The micro loading effect is prevented by a method that uses a metal layer, which is located on the glass surface and is electrically connected with the silicon substrate[10], as shown in Fig. 2(d). Aluminum bonding points 7 and 8 are connected ohmically by fixed combs. The picture of the U-shape beam, whose micro loading effect is prevented by this method, is shown in Fig. 7.

To validate that the sensing acceleration is due to the capacitance having variable overlap, and to experimentally verify the extent to which the noise is reduced by slide-film air damping, a device is fabricated. The SEM picture is shown in Fig. 8. The measurement of the quality factor was performed using an HP4395 A Network/Spectrum Analyzer and the capacitive accelerometer is caused to vibrate by using a small vibratory platform. The tested quality factor is as high as 514 when the packaging is done at room temperature and under atmospheric pressure. The corresponding mechanical noise of the resonator, having a mass of 2.79 mg, is $3.02 \times 10^{-2} \mu$g/$\sqrt{\text{Hz}}$, according to Eq. (2).
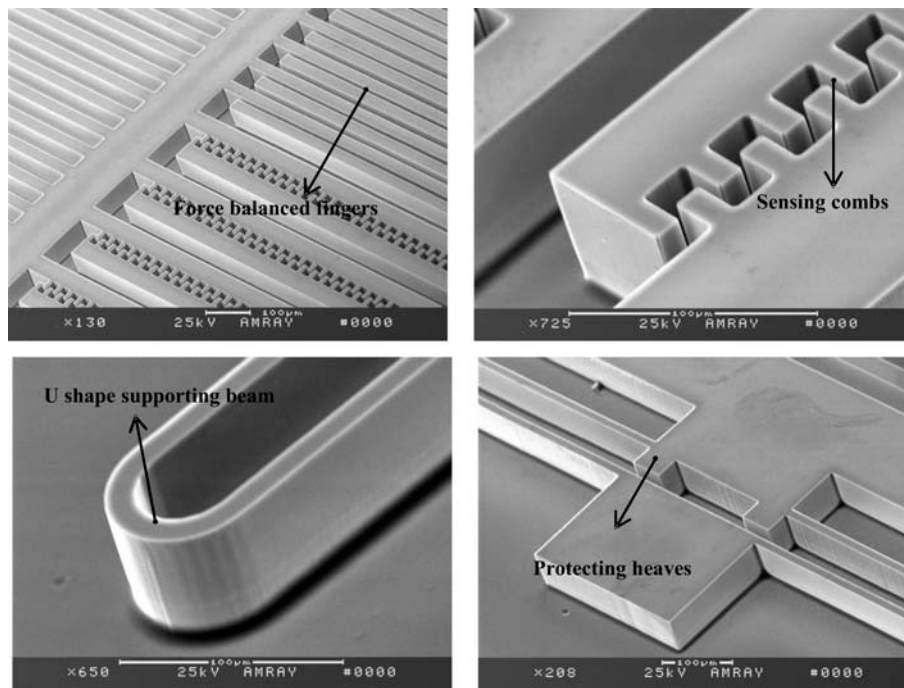
Fig. 7. SEM pictures of the fabricated inertial sensor chip.
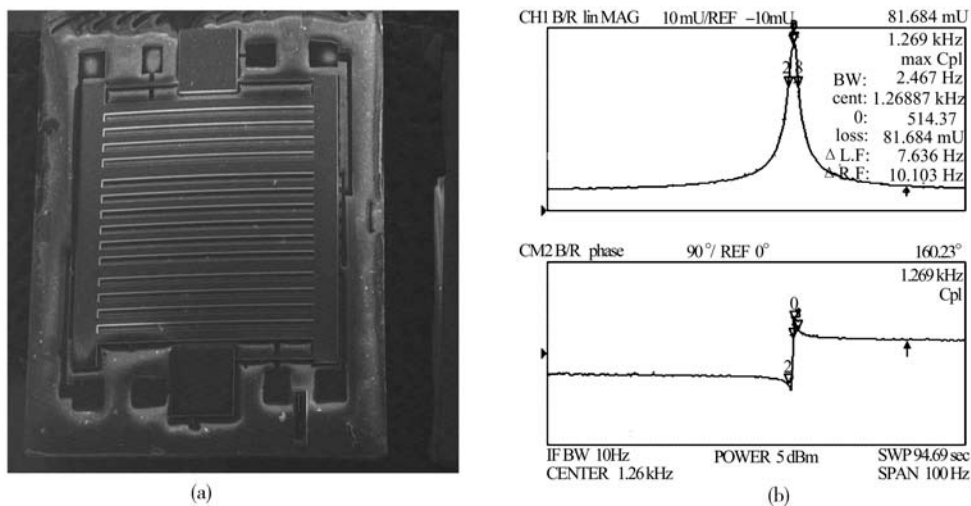
Fig. 8. (a) Picture of the device used for testing the slide-film damping; (b) Measured Q curves.

The sensitivity of the fabricated inertial sensor is also roughly measured. The tested inertial sensor, the circuit, and the test principle are shown in Fig. 9. An acceleration of 1 g is applied to the sensitive axis. The tested static line between the change of the sensing capacitance and the gravitational acceleration inertial is also shown in Fig. 9. Acceleration in the sensor's sensitive direction varies from 0 g to 1 g, when rotating the turntable from 0° to 180° in 15° steps. The sensitivity of the inertial sensor is determined to be 0.492 pf/g.

4. Summary

When the comb capacitances of MEMS comb capacitive accelerometers are fabricated by a DRIE process, the combs are usually not parallel for complicated process factors. The resolution of the traditional MEMS capacitive accelerometer is also restricted by the air damping of the MEMS structure and the voltage value of the alternative electric test signal.

Aiming at the disadvantage of traditional capacitive MEMS accelerometers, a novel MEMS capacitive accelerometer is designed and fabricated based on a silicon-glass bonding process. The accelerometer is analyzed by the FEM tool ANSYS. Both mechanical noise and electrical noise are reduced by the changed MEMS structure. The quality factor of the testing device is 514, which shows that the enhanced capacitors can reduce mechanical noise. The preliminary testing sensitivity of the accelerometer is as high as 0.492 pf/g.

Acknowledgment
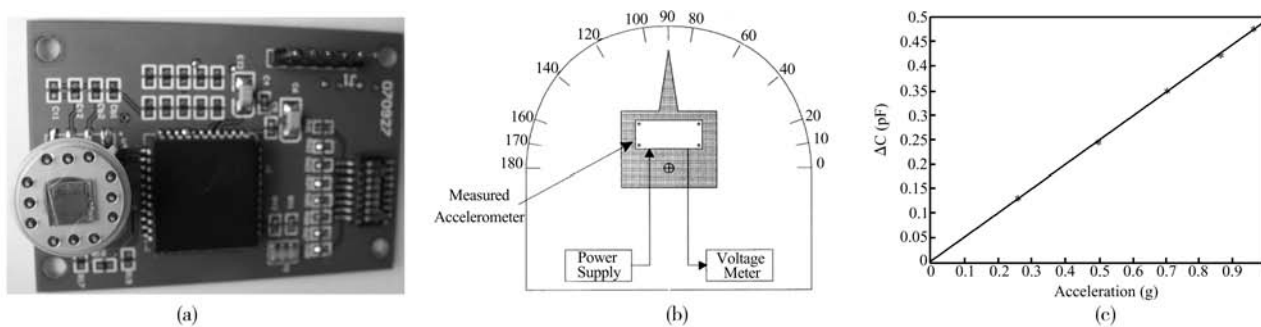
Fig. 9. Picture of (a) the sensor, (b) the interface circuit, and (c) the measured static line.

References

[1] Gabrielson T B. Mechanical-thermal noise in micromachined acoustic and vibration sensors. IEEE Trans Electron Devices, 1993, 40(5): 903

[2] Bordoni F. Noise in sensors. Sensors and Actuators, 1990, A21–23: 17

[3] Beliveau A, Spencer G T, Thomas K A, et al. Evaluation of MEMS capacitive accelerometer. IEEE Design Test Comput, 1999, 16: 48

[4] Dong L, Che L, Sun L, et al. Effects of non-parallel combs on reliable operation conditions of capacitive inertial sensor for step and shock signals. Sensors and Actuators A, 2005, 121(2): 395

[5] Han K H, Cho Y H. Self-balanced navigation-grade capacitive microaccelerometers using branched finger electrodes and their performance for varying sense voltage and pressure. Journal of MEMS, 2003, 12(1): 11

[6] Bao M. Handbook of sensors and actuators series: micro mechanical transducer. Vol. 8. 1st ed. Elsevier, 2000: 123

[7] Tay F E H, Xu J, Liang Y C, et al. The effects of non-parallel plates in a differential capacitive microaccelerometer. Journal of Micromechanical and Microengineering, 1999, 9: 283

[8] Dong Linxi, Yan Haixia, Qian Xian, et al. Study of inertial pulse response of MEMS capacitive accelerometer with non-parallel combs. Chinese Journal of Electronics, 2008, 36(5): 1035

[9] Petersen K E. Silicon as a mechanical material. Proc IEEE, 1982, 70: 420

[10] Chabloz M, Jiao J, Yoshida Y, et al. A method to evade microloading effect in deep reactive ion etching for anodically bonged glass-silicon structures. Proc IEEE Micro ElectroMechanical System Workshop, Miyazaki, Japan, 2000